Light scattering by multi-layered axisymmetric particles

V G Farafonov†, M S Prokopjeva‡ and V B Il'in‡

† St.Petersburg University of Aerocosmic Instrumentation, Bol.Morskaya ul. 67, St.Petersburg 190000, Russia
‡ Sobolev Astronomical Institute, St.Petersburg University, Bibliotechnaya pl. 2, St.Petersburg 198504, Russia

E-mail: vi2087@vi2087.spb.edu

Abstract. We present an exact solution to the problem of light scattering by multi-layered axisymmetric particles and a numerical code implementing this solution. The main features of the solution are: separation of the incident, scattered, and internal fields into two parts with a proper choice of scalar potentials for each of them, expansion of the potentials in terms of the spherical wave functions, usage of surface integral equations and truncated systems of linear algebraic equations relative to the coefficients of the potential expansions. The solution is also formulated in a recursive way.

The numerical code developed has shown that the solution really allows a treatment of axisymmetric particles of quite different internal structures (e.g., combinations of a spherical core, a prolate spheroidal layer and an oblate spheroidal mantle). Some illustrative results of calculations of the optical properties of layered particles are given and briefly discussed.

Submitted to: *Meas. Sci. Technol.*

1. Introduction

Various natural scatterers are known to have an internal structure. Therefore, the problem of light scattering by inhomogeneous particles is of great interest for different scientific fields – atmosphere and ocean optics, biophysics, astrophysics, etc. In many cases inhomogeneous dust grains can be well represented by multi-layered particles.

To simulate light scattering by such particles one usually utilizes the model of multi-layered spheres based on a relatively simple and effective algorithm [1]. Different approaches allow one to solve the problem of light scattering by multi-layered *non-spherical* particles – the separation of variables method (SVM), the T-matrix method (TMM), the discrete dipole approximation (DDA) and many others (see, e.g., [2]). But till now consideration was mainly restricted to core-mantle particles: spheroids treated by the SVM [3, 4, 5, 6], axisymmetric particles by the TMM [7, 8], ellipsoids by the DDA [9], etc. Non-spherical particles with 3 and more layers were studied mainly theoretically (without any numerical results) by the SVM [10, 11], the TMM [7, 12] (except for [7], where calculations for three-layered spheroids were done) and so on.

In this paper we describe a new recursive solution to the problem of light scattering by multi-layered axisymmetric particles. The solution was embodied into a numerical code and some results obtained for multi-layered particles are shortly discussed.

2. Basic equations

Let us consider scattering of a plane wave incident at an n-layered axisymmetric particle. The particle geometry is defined by the layer surface equations

$$r^{(j)}(\theta) = 0, \qquad j = 1, 2, ..., n, \tag{1}$$

where θ is one of the angles of the spherical coordinate system connected with the particle. The surfaces are assumed to have no common points.

The fields in the j-th layer bounded by the surfaces $r^{(j)}(\theta) = 0$ and $r^{(j+1)}(\theta) = 0$ are denoted by $\boldsymbol{E}^{(j+1)}, \boldsymbol{H}^{(j+1)}$. Thus, $j = 1$ corresponds to the outermost layer (a mantle of the particle) and $j = n$ to the innermost layer (a core). As in the case of a homogeneous particle, $\boldsymbol{E}^{(0)}, \boldsymbol{H}^{(0)}$ and $\boldsymbol{E}^{(1)}, \boldsymbol{H}^{(1)}$ are the incident and scattered fields, respectively.

Maxwell's equations with boundary conditions at each layer surface along with the radiation condition at infinity are to be solved (see, e.g., [13]). To do that, our approach developed earlier in [14, 15, 16] for homogeneous axisymmetric particles is applied. The main features of the approach are as follows.

All the fields are divided into two parts – *axisymmetric*, independent of the azimuthal angle φ, and *non-axisymmetric*, with an average, taken over φ, of zero (see [17] about the possibility of such field separation):

$$\boldsymbol{E}^{(j)} = \boldsymbol{E}_{\rm A}^{(j)} + \boldsymbol{E}_{\rm N}^{(j)}, \qquad \boldsymbol{H}^{(j)} = \boldsymbol{H}_{\rm A}^{(j)} + \boldsymbol{H}_{\rm N}^{(j)}, \tag{2}$$

where $j = 0, 1, ..., n+1$.

The light scattering problem is solved independently for each of the parts utilizing different scalar potentials. Such an approach generally allows a treatment of non-spherical particles in a more adequate way than is done by the standard methods (see [18, 19] for more details).

2.1. Axisymmetric parts

The azimuthal components of the fields are used here as scalar potentials

$$p^{(j)} = E^{(j)}_{\mathrm{A},\varphi} \cos\varphi, \qquad q^{(j)} = H^{(j)}_{\mathrm{A},\varphi} \cos\varphi, \tag{3}$$

where $j = 0, 1, ..., n+1$. Other components of the fields can be expressed via the azimuthal components (and hence the potentials) using Maxwell's equations. The potentials p and q are connected with the TE and TM modes, respectively.

For each layer, we represent the scalar potential p as a sum

$$p^{(j)} = \tilde{p}^{(j)}_1 + \tilde{p}^{(j)}_2, \tag{4}$$

where $\tilde{p}^{(j)}_1$ has no peculiarity at the origin of the coordinate system, $\tilde{p}^{(j)}_2$ satisfies the radiation condition at infinity. Note that $\tilde{p}^{(n+1)}_1 = p^{(n+1)}$, $\tilde{p}^{(n+1)}_2 = 0$ and equation (4) can be considered for $j = 1, 2, .., n+1$, if one introduces the following notations: $\tilde{p}^{(1)}_1 = p^{(0)}$, $\tilde{p}^{(1)}_2 = p^{(1)}$. The same is done with the potential q. Evidently, all the potentials $(p, \tilde{p}, q, \tilde{q})$ satisfy the scalar Helmholtz equation.

The problem is formulated in the form of surface integral equations. After substitution of the boundary conditions into the integral equations equivalent to the Helmholtz equation and simple transformations we get

$$\int_{S_j} \Bigg\{ p^{(j+1)}(\boldsymbol{r}') \frac{\partial G(k_j, \boldsymbol{r}, \boldsymbol{r}')}{\partial n} - \Bigg[\frac{\mu_j}{\mu_{j+1}} \frac{\partial p^{(j+1)}(\boldsymbol{r}')}{\partial n} + \left(\frac{\mu_j}{\mu_{j+1}} - 1 \right) \frac{1}{\sqrt{(r')^2 + \left[(r')'_{\theta'}\right]^2}} \cdot$$
$$\cdot \left(1 - \frac{(r')'_{\theta'}}{r'} \mathrm{ctg}\theta' \right) p^{(j+1)}(\boldsymbol{r}') \Bigg] G(k_j, \boldsymbol{r}, \boldsymbol{r}') \Bigg\} dS' = \begin{cases} -\tilde{p}^{(j)}_1(\boldsymbol{r}), & \boldsymbol{r} \in D_j, \\ \tilde{p}^{(j)}_2(\boldsymbol{r}), & \boldsymbol{r} \in R^3 \setminus \bar{D}_j, \end{cases} \tag{5}$$

where $p^{(j+1)} = \tilde{p}^{(j+1)}_1 + \tilde{p}^{(j+1)}_2$ and $j = 1, 2, ..., n$. Similar equations can be obtained for the potentials $\tilde{q}^{j+1}_1$, $\tilde{q}^{j+1}_2$.

The scalar potentials are expanded in terms of the spherical wave functions

$$\begin{matrix} \tilde{p}^{(j)}_1 \\ \tilde{q}^{(j)}_1 \end{matrix} = \sum_{l=1}^{\infty} \begin{matrix} a^{(j)}_{l,1} \\ b^{(j)}_{l,1} \end{matrix} \; j_l(k_j r) \; P^1_l(\cos\theta) \; \cos\varphi, \tag{6}$$

where $j_l(k_j r)$ is the Bessel function, $P^1_l(\cos\theta)$ the associated Legendre function, $j = 1, 2, ..., n+1$. The potentials $\tilde{p}^{(j)}_2, \tilde{q}^{(j)}_2$ are expanded in the same way, but $j_l(k_j r)$ should be replaced with the Hankel function of the first kind $h^{(1)}_l(k_j r)$. The expansion of the Green function is well known (see, e.g., [20]).

All expansions are substituted into the surface integral equations (5). Due to the orthogonality of the spherical wave functions, one gets two infinite systems of algebraic equations relative to the coefficients of the potential expansions. Solution of the systems for the TE mode gives the coefficients for the scattered field $\boldsymbol{a}^{(1)} = \{a_{l,2}^{(1)}\}_{l=1}^{\infty}$ in the form typical of the TMM

$$\boldsymbol{a}^{(1)} = A_2 \cdot A_1^{-1} \, \boldsymbol{a}^{(0)}, \tag{7}$$

where $\boldsymbol{a}^{(0)} = \{a_{l,1}^{(1)}\}_{l=1}^{\infty}$ are known coefficients for the incident field (a plane wave), and the matrices A_1 and A_2 are determined as follows:

$$\begin{pmatrix} A_1 \\ A_2 \end{pmatrix} = \begin{pmatrix} -A_{\rm hj}^{(1)} & -A_{\rm hh}^{(1)} \\ A_{\rm jj}^{(1)} & A_{\rm jh}^{(1)} \end{pmatrix} \cdot \ldots \cdot \begin{pmatrix} -A_{\rm hj}^{(n-1)} & -A_{\rm hh}^{(n-1)} \\ A_{\rm jj}^{(n-1)} & A_{\rm jh}^{(n-1)} \end{pmatrix} \cdot \begin{pmatrix} -A_{\rm hj}^{(n)} \\ A_{\rm jj}^{(n)} \end{pmatrix}. \tag{8}$$

Here $A_{\rm hj}^{(j)}$ is a matrix whose elements are surface integrals of products of the spherical wave functions and their derivatives calculated for the j-th layer (see [13] for more details). The subscripts j, h show what radial functions are used in the integrals – the Bessel (j) or Hankel (h) one. Solution for the TM mode is analogous.

2.2. Non-axisymmetric parts

Superpositions of vertical components of the Hertz vector $U^{(j)}$ and the Debye potentials $V^{(j)}$ ($j = 0, 1, ..., n$) are selected as scalar potentials here. For instance, for the TE mode we have

$$\begin{aligned} \boldsymbol{E}_{\rm N}^{(j)} &= \nabla \times \left(U^{(j)} \, \boldsymbol{i}_{\rm z} + V^{(j)} \, \boldsymbol{r}\right), \\ \boldsymbol{H}_{\rm N}^{(j)} &= \frac{1}{i\mu_j k_0} \nabla \times \nabla \times \left(U^{(j)} \, \boldsymbol{i}_{\rm z} + V^{(j)} \, \boldsymbol{r}\right), \end{aligned} \tag{9}$$

where $\boldsymbol{r}$ is the radius-vector, $\boldsymbol{i}_{\rm z}$ a unit vector of the Cartesian system connected with the particle, μ_j magnetic permeability of the j-th layer, k_0 wavenumber in vacuum. Expressions for the TM mode are similar (see, e.g., [15]).

The next steps are in general similar to those made for the axisymmetric part in section 2.1. We represent the scalar potentials for each layer as sums

$$U^{(j)} = \tilde{U}_1^{(j)} + \tilde{U}_2^{(j)}, \quad V^{(j)} = \tilde{V}_1^{(j)} + \tilde{V}_2^{(j)}, \tag{10}$$

where $j = 1, 2, ..., n+1$.

Substitution of corresponding boundary conditions in the surface integral equations leads to integral equations resembling those for the axisymmetric parts (see equation (5)).

The potentials are expanded in terms of the spherical wave functions

$$\begin{matrix} \tilde{U}_1^{(j)} \\ \tilde{V}_1^{(j)} \end{matrix} = \sum_{m=1}^{\infty} \sum_{l=m}^{\infty} \begin{matrix} a_{ml,1}^{(j)} \\ b_{ml,1}^{(j)} \end{matrix} \; j_l(k_j r) \; P_l^m(\cos\theta) \; \cos m\varphi, \tag{11}$$

where $j = 1, 2, ..., n+1$. The expressions for the potentials with the subscript 2 are the same after the replacement of $j_l(k_j r)$ with $h_l^{(1)}(k_j r)$.

Substitution of the expansions into the surface integral equations gives for each m two infinite systems of algebraic equations relative to the coefficients of the potential expansions. Solution of the systems provides the coefficients for the scattered field

$\boldsymbol{a}_m^{(1)} = \{a_{ml,2}^{(1)}\}_{l=1}^{\infty}, m \geq 1$ in the form (7)–(8) with the only difference – the matrices $A^{(j)}$ will have a block structure, namely:

$$A_{hj}^{(j)} = \begin{pmatrix} \alpha_{\mathrm{hj},1}^{(j)} & \beta_{\mathrm{hj},1}^{(j)} \\ \alpha_{\mathrm{hj},2}^{(j)} & \beta_{\mathrm{hj},2}^{(j)} \end{pmatrix}, \tag{12}$$

where $\alpha_{\mathrm{hj},i}^{(j)}$ and $\beta_{\mathrm{hj},i}^{(j)}$ are matrices whose elements are surface integrals of products of the spherical wave functions and their derivatives calculated for the j-th layer (see [13] for more details).

The systems arising for axisymmetric and non-axisymmetric parts were investigated analytically and numerically in the case of homogeneous particles [21]. It was found that they had similar properties and affected the range of applicability of the method nearly in the same way.

2.3. Recursive form

The most essential part of the solution for both the axisymmetric and non-axisymmetric parts – equation (8) – can be written in the recursive form

$$\begin{pmatrix} A_{1,n+1} \\ A_{2,n+1} \end{pmatrix} = \begin{pmatrix} -A_{\mathrm{hj}}^{(1)} & -A_{\mathrm{hh}}^{(1)} \\ A_{\mathrm{jj}}^{(1)} & A_{\mathrm{jh}}^{(1)} \end{pmatrix} \cdot \begin{pmatrix} A_{1,n} \\ A_{2,n} \end{pmatrix}, \tag{13}$$

where the right-hand side vector contains the values of A_1, A_2 for a given n-layered particle, the matrix corresponds to the new outer layer, and the left-hand side vector gives the values for a new $(n+1)$-layered particle formed in this way.

Equation (13) can be rewritten in another way

$$T_{n+1} = \left(A_{\mathrm{jj}}^{(1)} + A_{\mathrm{jh}}^{(1)} \cdot T_n\right) \left(A_{\mathrm{hj}}^{(1)} + A_{\mathrm{hh}}^{(1)} \cdot T_n\right)^{-1}, \tag{14}$$

where $T_n = A_{2,n} \cdot A_{1,n}^{-1}$. This equation is equivalent to that obtained for multi-layered axisymmetric particles in [7]. Although equation (13) looks less exciting, it should be preferred to equation (14) as the former needs only one matrix inversion ($T_{n+1} = A_{2,n+1} \cdot A_{1,n+1}^{-1}$), whereas the latter requires inversions for each layer and one more at the last step.

We have suggested a similar approach for multi-layered spheroidal particles within the separation of variables approach [11]. Unlike the recent similar work [10], our SVM approach involves *linear* algebraic equations for the coefficients of potential expansions and hence seems to be more perspective.

3. Numerical results

We have developed a computer code implementing the approach and tested it in different ways (see, e.g., [22]). Comparison with available codes for multi-layered spheres [23] and core-mantle confocal spheroids [5] and the modified DDA code [9] for multi-layered non-confocal ellipsoids (and spheroids) gave good results in all the cases. It is, however, too early to discuss the range of applicability of our approach and code – we need to complete analytical and numerical investigations like those made for the method in the case of homogeneous particles [21]. At the moment, we are working at a test version of the code, which will be improved in several places before public release. However, already this version allows us to treat scatterers with the diffraction parameter as large as $x_{\rm V} \approx$5–7 ($x_{\rm V} = 2\pi r_{\rm V}/\lambda$, where $r_{\rm V}$ is the radius of the equivolume sphere, λ the wavelength of incident radiation) and to reach, in some cases, the applicability limits of our more elaborated "core-mantle" SVM code [5]. We mention in passing, that work with this SVM code made us thinking that the new code would be inapplicable to particles with thin layers (some of the approaches used in the codes are similar), but it does work. This opens a possibility for the new code to treat particles with nearly smooth internal changes of the optical constants.

The influence of internal structure (in the form of layers) of scatterers on their optical properties for core-mantle spheroids has been discussed by Onaka [3] and Farafonov and co-authors [5]. They considered the effect of variations of the refractive index m, the aspect ration a/b and other parameters of the mantle and the core. The SVM method utilized in both cases limited the analysis to spheroids with confocal layers. The confocality essentially restricts the internal structure of particles – the shape of the core is uniquely determined by its volume. Therefore, in discussion of figures 1–6 illustrating work of the new code we mainly concentrate on the effects of the layer shape.

In figure 1 we consider the scattering cross-section $C_{\rm sca}$ normalized by the geometrical cross-section of the equivolume sphere ($\pi r_{\rm V}^2$) for core-mantle non-confocal spheroids and change either the shape of the mantle or that of the core. One can see that in the region of the first maximum of $C_{\rm sca}(x_{\rm V})$ variations of the mantle shape have an observable effect (upto 35–40%), whereas variations of the core shape do not. This simple example illustrates a common situation – for a layered particle, nearly always there are one or a few layers dominating the scattering process. To a first approximation, such "main" layers can apparently be identified as those having the maximum $|m-1|\,V$, where m and V are the refractive index and the volume of a layer. For particles examined in figure 1, the mantle, due to its large volume, dominates and hence its shape determines the behaviour of the cross-section.

It should be noted that for multi-layered particles the condition defining the main layers can be complicated by such effects as screening, focussing, etc. (see, e.g., [5]). An example is given by a comparison of figures 1 and 2: for a spherical mantle, there is no dependence on the core shape, whereas for a (prolate/oblate) spheroidal mantle this dependence appears. Note also that scattering (extinction) at the first interference maximum is higher for particles with a prolate core and a prolate mantle than for an oblate core and an oblate mantle (at least, for a nearly axial incidence of radiation that we considered).

The situation when the core is more important than the mantle is presented in figure 3. To achieve this, we increased the refractive index of the core. As a result the mean refractive index of the particle became large and the regular interference maxima and minima were distorted by strong ripples. When the normalized cross-sections were

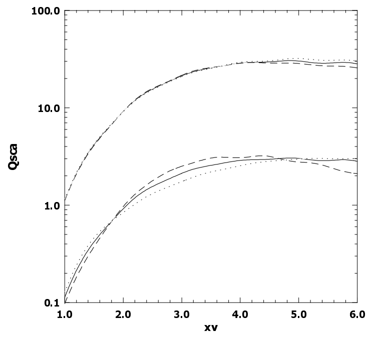

Figure 1. Normalized scattering cross-section $Q_{\rm sca}$ of core-mantle spheroids as a function of $x_{\rm V}$. The refractive indices are: $m_{\rm c} = 1.7$ (core), $m_{\rm m} = 1.3$ (mantle); the core volume fraction is $V_{\rm c}/V_{\rm tot} = 0.125$. Radiation is incident at $\alpha = 1°$ angle. Three *lower* curves show the values for particles with a spherical core and different mantles: oblate spheroid (dotted line), sphere (solid line), prolate spheroid (dashed line). Three *upper* curves present the values (multiplied by 10) for particles with a spherical mantle and different cores: oblate spheroid (dotted line), sphere (solid line), prolate spheroid (dashed line). All spheroids have the aspect ratio a/b =1.4.

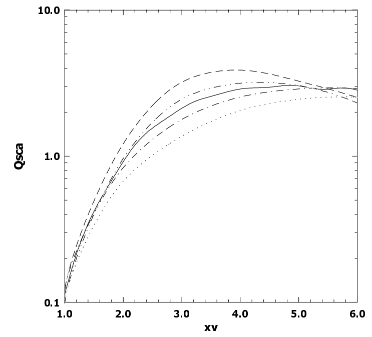

Figure 2. The same as in figure 1, but for spheroids with the following combinations core/mantle (S stands for sphere, P for prolate and O for oblate spheroids): P/P (dashed line), O/P (double-dot-dashed line), S/S (solid line), P/O (dot-dashed line), O/O (dotted line).

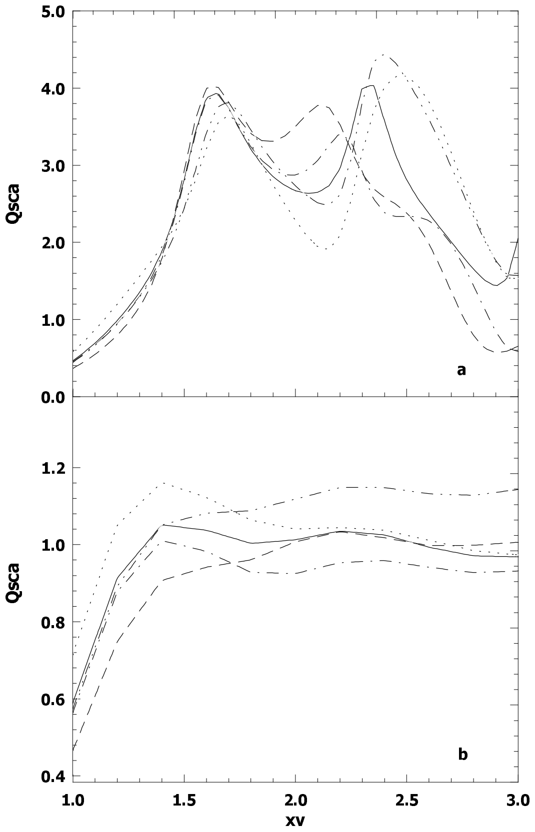

Figure 3. The same as in figure 2, but for other core volume fraction $V_c/V_{\rm tot} = 0.343$ and other refractive indices: **a** – $m_{\rm c} = 2.5$ (core), $m_{\rm m} = 1.3$ (mantle); **b** – $m_{\rm c} = 2.5 + 1.5{\rm i}$ (core), $m_{\rm m} = 1.3 + 0.01{\rm i}$ (mantle).

plotted against the phase shift of the central ray ρ (see, e.g., [24]), we did not observe the coincidence of the interference maxima positions for different core-mantle particles, contrary to [3, 5]. We give the dependence of $Q_{\rm sca}$ on $x_{\rm V}$ also because, in this case, the difference of the ripple structures is better seen and the behaviour of the curves in the region $x_{\rm V} < 1$ is obvious and therefore this region can be skipped in figures.

It should be emphasized that the ripples of the curves plotted in figure 3a strongly depend not only on the shape of the main layer (core), but also on the shape of the optically thin layer (mantle). This effect is well seen in figure 4 where three-layer particles with a complex structure are presented – changes of the shapes of the outer boundaries of the vacuum layer and icy-like mantle (both layers give very small contributions to the phase shift of the central ray and a volume-average refractive index), significantly affect the ripple structure. Note also that for absorbing layered particles presented in figure 3b the behaviour of $Q_{\rm sca}$ depends on the mantle shape as well.

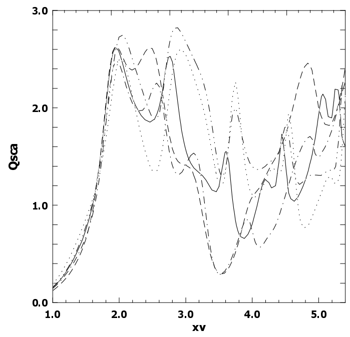

Figure 4. Normalized scattering cross-section $Q_{\rm sca}$ of three-layered spheroids as a function of $x_{\rm V}$. The refractive indices are: $m_{\rm c} = 2.5$ (core), $m_{\rm l} = 1.0$ (layer), $m_{\rm m} = 1.3$ (mantle); the volume fractions are: $V_{\rm c}/V_{\rm tot} = 0.216$ (core), $V_{\rm l}/V_{\rm tot} = 0.296$ (layer). The following core/layer/mantle combinations are shown (notations as in figure 3): S/S/S (solid line), P/P/P (dashed line), P/S/O (dot-dashed line), O/O/O (dotted line), O/S/P (double-dot-dashed line). All spheroids have the aspect ratio a/b =1.4.

4. Conclusions

We have developed a new method and a code to solve the problem of light scattering by multi-layered axisymmetric particles. The theoretical solution is formulated in the recursive form and the algorithm is found to be stable for (very) thin layers. This makes the approach potentially useful for studies of particles with complex internal variations of the optical constants.

Presented results of illustrative calculations made for particles with a few layers were used to draw some conclusions on the influence of the layer shapes on the first interference maximum and ripple structures. A detailed consideration of the dependence of the optical properties of multi-layered non-spherical particles on their internal structure will be done elsewhere.

Acknowledgments

The authors are thankful to N.V.Voshchinnikov and N.A.Krivova for many remarks and suggestions that improved the text. The work was supported by the INTAS (grant 99/652) and by the Russian federal government (within the programme "Astronomy").

References

[1] Wu Z P and Wang Y P 1991 *Radio Science* **26** 1393

[2] Mishchenko M I, Hovenier J W and Travis L D 2000 *Light Scattering by Non-Spherical Particles* (San Diego: Acad. Press)
[3] Onaka T 1980 *Ann. Tokyo Astron. Obs.* **18** 1
[4] Cooray M F R and Ciric I R 1992 *J. Electr. Waves Appl.* **6** 1491
[5] Farafonov V G, Voshchinnikov N V and Somsikov V V 1996 *Appl. Opt.* **35** 5412
[6] Voshchinnikov N V 1996 *J. Quant. Spectr. & Rad. Transf.* **55** 627
[7] Wang D S and Barber P W 1979 *Appl. Opt.* **18** 1190
[8] Wang D S, Chen H C, Barber P W and Wyatt P J 1979 *Appl. Opt.* **18** 2672
[9] Draine B T and Flatau P 1999 *Preprint Princeton Obs.* POPe-785
[10] Gurwich I, Kleiman M, Shiloah N and Cohen A 2000 *Appl. Opt.* **39** 470
[11] Farafonov V G 2001 *Opt. Spectrosc.* **90** 743
[12] Peterson B and Strom S 1974 *Phys. Rev. D* **10** 2670
[13] Farafonov V G 2001 *Opt. Spectrosc.* **91** in press
[14] Farafonov V G 2000 *Opt. Spectrosc.* **88** 70
[15] Farafonov V G, Il'in V B and Henning T 1999 *J. Quant. Spectr. & Rad. Transf.* **63** 205
[16] Farafonov V G and Il'in V B 2001 *Opt. Spectrosc.* **91** in press
[17] Farafonov V G and Slavyanov S Yu 1980 *Radiotechnics and Electronics (Sov.)* **25** 2056
[18] Farafonov V G 1983 *Differential Equations (Sov.)* **19** 1765
[19] Voshchinnikov N V and Farafonov V G 1993 *Astrophys. Space Sci.* **204** 19
[20] Morse P M and Feshbach H 1953 *Methods of Theoretical Physics* (New York: McGraw-Hill)
[21] Farafonov V G 2001 *Opt. Spectrosc.* submitted
[22] Farafonov V G and Il'in V B 2001 *Meas. Sci. Technol.* this issue
[23] Voshchinnikov N V and Mathis J S 1999 *Astrophys. J.* **526** 257
[24] Kokhanovsky A A 1999 *Light Scattering Media Optics: Problems and Solutions* (Chichester: Wiley-Praxis)